ACS Partner Journal

ENVIRONMENT & HEALTH

Editors' Choice

Open Access

pubs.acs.org/EnvHealth

Article

MPs Entering Human Circulation through Infusions: A Significant Pathway and Health Concern

Tingting Huang,[#] Yangyang Liu,[#] Licheng Wang,[#] Xuejun Ruan,[#] Qiuyue Ge, Minglu Ma, Wei Wang, Wenbo You, Liwen Zhang, Ventsislav Kolev Valev,[*] and Liwu Zhang[*]

Cite This: *Environ. Health* 2025, 3, 551−559

Read Online

ACCESS | Metrics & More | Article Recommendations | Supporting Information

ABSTRACT: Human uptake of microplastic particles (MPs) is causing increasing health concerns, and there is mounting pressure to evaluate the associated risks. While MPs can be ingested, breathed in, or drank in, a very direct entrance channel is available through ingress into the bloodstream. Intravenous infusion usually proceeds from plastic bottles. Many are made of polypropylene (PP), and filtering is applied to limit particle contamination. In this study, we examined the MPs' content of filtrates using a combination of surface-enhanced Raman spectroscopy and scanning electron microscopy. We find that the number of PP particles is significant (~7500 particles/L). The MP sizes range from 1 to 62 μm, with a median of ~8.5 μm. About 90% of particles ranged between 1 and 20 μm in size, with ~60% in the range 1 to 10 μm. We then discuss the potential number of such particles injected and the consequences of their presence in the bloodstream. We highlight the organs for potential deposition, and we discuss possible clinical effects. Our quantitative data are important to help evaluate the toxicity risks associated with MPs and to accurately balance those risks versus the benefits of using intravenous injections.

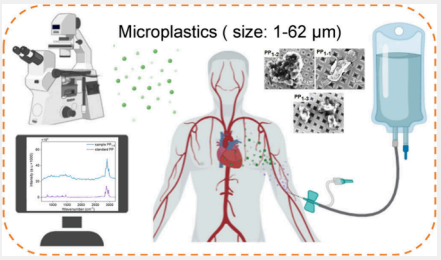

KEYWORDS: *MPs, intravenous infusion, health concerns, PP, particle contamination, SERS*

1. INTRODUCTION

Plastic pollution has become a global challenge. Plastics started to be mass-produced in the 1950s,[1] and in the last 50 years, production has increased over 20 times,[2] reaching 359 million tons in 2018.[3] Each year, between 8 and 10 million tons of plastic are estimated to enter the global ocean, for a total plastic waste approximating 5 billion tons, for now.[1,4,5] In the oceans, plastic accounts for 73% of debris,[4] which was first reported to affect marine living organisms in 1972.[6,7] The most abundant forms of debris are nanoplastics (<0.1 μm) and microplastics (<5 mm).[8] There are two types of microplastic particles (MPs). Primary MPs are intentionally manufactured small polymer particles, such as preproduction pellets or microbeads, which are used in products like abrasives, paints, and other industrial applications.[9] However, recent regulations have restricted the use of primary MPs in cosmetics, drastically reducing their presence in these products.[10] Secondary MPs, on the other hand, are formed through the degradation of larger plastics due to factors like UV light exposure, physical abrasion, temperature changes, hydrolysis, or biodegradation.[11]

Although various analytical techniques, such as Fourier transform infrared spectroscopy (FT-IR) and Raman spectroscopy, as well as other methods like pyrolysis gas chromatography−mass spectrometry (PyGC-MS) and liquid chromatography−tandem mass spectrometry (LC-MS/MS), have been widely applied in plastic pollution analysis, they differ in sensitivity, resolution, and operational complexity.[12−14] Moreover, these methods often lack sufficient sensitivity and specificity for detecting micro- and nanoscale particles. Consequently, data obtained from different studies using these techniques may be challenging to compare directly, affecting the consistency and standardization of MP data. Surface-enhanced Raman spectroscopy (SERS) has emerged as a promising analytical technique for the detection and characterization of MPs and nanoplastic particles (NPs).[15] SERS combines the advantages of Raman spectroscopy with plasmonic effects induced by metallic nanostructures, resulting in significantly enhanced signal intensities.[16] This technique enables the detection of low concentrations of plastic particles and provides valuable chemical information regarding the molecular composition of the detected particles.[17]

While MPs can serve as vectors for chemical toxins,[18] many of their effects are due to physical properties, such as shape and size.[19] Once ingested, MPs can translocate into the circulatory system and the tissues, where their effects include inflammatory responses and necrosis.[20] As these particles can be ingested,[21,22] inhaled,[23,24] or imbibed by humans, there is increasing concern for human health.[1,3,25,26] The reason for concern is acute in the case of the direct intravenous injection

Received: October 8, 2024
Revised: December 23, 2024
Accepted: December 24, 2024
Published: February 14, 2025

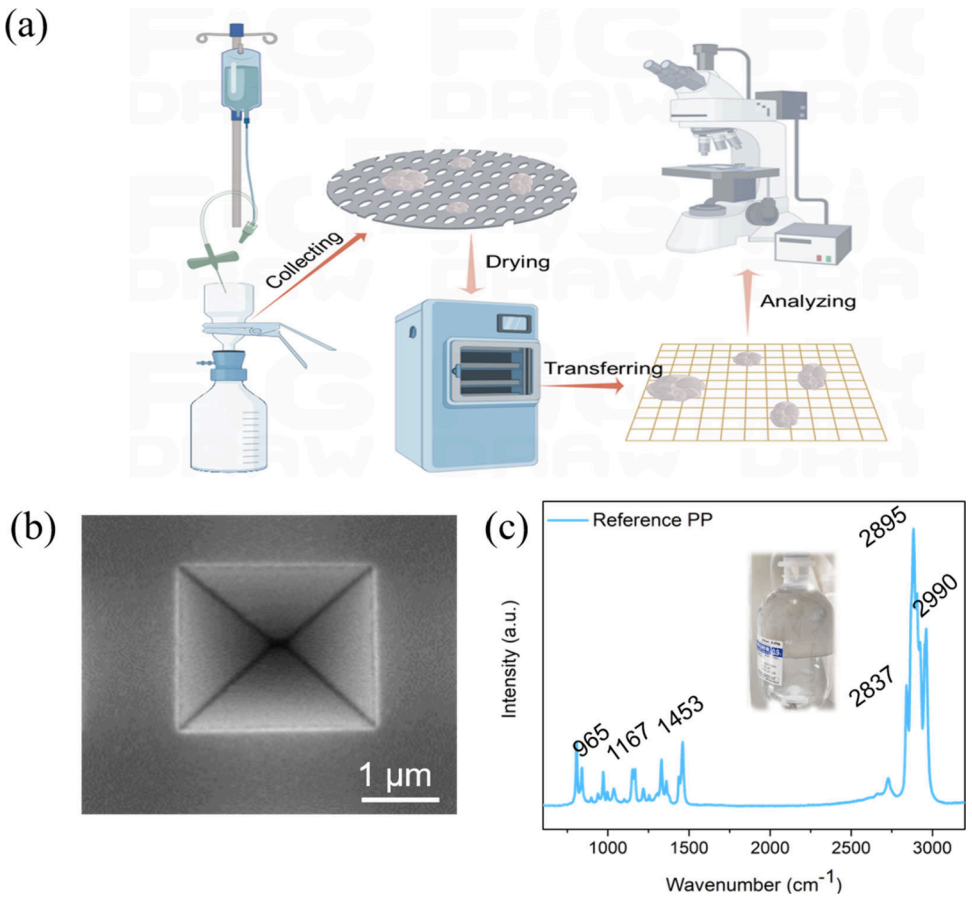

Figure 1. Procedure for detecting microplastic particles (MPs) inside fluids from infusion bottles. (a) The experiment follows the clinical intravenous infusion process. Particles were enriched on a filter membrane. Then, after ultrasonication, the solution was heated and concentrated in an oven, prior to being dripped onto the homemade substrate for surface-enhanced Raman scattering (SERS) analysis. (b) Top-view scanning electron microscopy (SEM) image of the V-shaped Si−Au substrate. The structure of the substrate is that of an inverted pyramid. (c) The Raman spectrum of the infusion bottle itself, which is made of polypropylene (PP).

of MPs. Although plastic particles in commercially available infusion fluids were reported in 1970,[27] this pioneering work has attracted very little attention. Evidence for the clinical significance of such particles in the human bloodstream was already available in the 70s,[28] and recent reports concur.[29] In 2022, Leslie et al. were the first to detect micro/nanoplastic particles (M/NPs) larger than 700 nm in the blood of healthy individuals using Py-GC/MS, with a concentration of 1.6 μg/L, predominantly composed of polyethylene (PE), polystyrene (PS), and polyethylene terephthalate (PET),[30] and their presence has been confirmed in infusion systems and bottles.[14,31] Gopinath et al. also described the administration of M/NPs and additives through ingestion, inhalation, infusion, and dermal routes via medical devices and reviewed the mechanisms of interaction between pharmaceutical ingredients and M/NPs additives. They highlighted that M/NPs or their leachates can interact with blood components, such as red and white blood cells, platelets, and plasma proteins, potentially causing cytotoxic and genotoxic effects.[32] However, as we have seen above, the toxicity of MPs is related to their size. Yet understanding of the size distribution of MPs in infusion bottles is currently lacking.

Here, we employed a combination of optical and electron microscopy techniques to identify, count, and measure MPs from infusion bottle fluids; six polypropylene (PP) bottles were studied from two brands. Specifically, SERS was used to confirm that the counted particles were made of PP. We report the presence of ~7,500 such microparticles per liter of fluid. The vast majority (~90%) of particles ranged between 1 and 20 μm in size, with ~60% of the particles in the range 1 to 10 μm. Crucially, our analysis was performed after the fluids were filtered by a common filtration system used for intravenous injections; therefore, the particles observed here have direct access to the human bloodstream. We discuss the importance of our findings in terms of the usual volumes of infusion fluids administrated, presence into the human bloodstream, deposition in various organs and resulting clinical effects.

2. METHODS AND MATERIALS

2.1. Chemicals and Materials

The filter consisted of polycarbonate filter paper (0.2 μm) purchased from Whatman. (The filtering material is consistent with the commonly used filtering material in clinical intravenous infusion.)[33] Medical saline solution (sodium chloride, 0.9%) packed with PP material was purchased from Henan Kellen Pharmaceutical Company and Guangxi Yuyuan Pharmaceutical Company. MPs detected from the above two brands were named 1 and 2, respectively. Deionized water was used after filtration throughout the experiments.

2.2. MPs Sample Preparation

Two brands (1 and 2) of saline infusion bottles made of PP material were used (250 mL in volume) and infused into a beaker at a common intravenous infusion rate of 40−60 drops/min through an

https://doi.org/10.1021/envhealth.4c00210
Environ. Health 2025, 3, 551−559

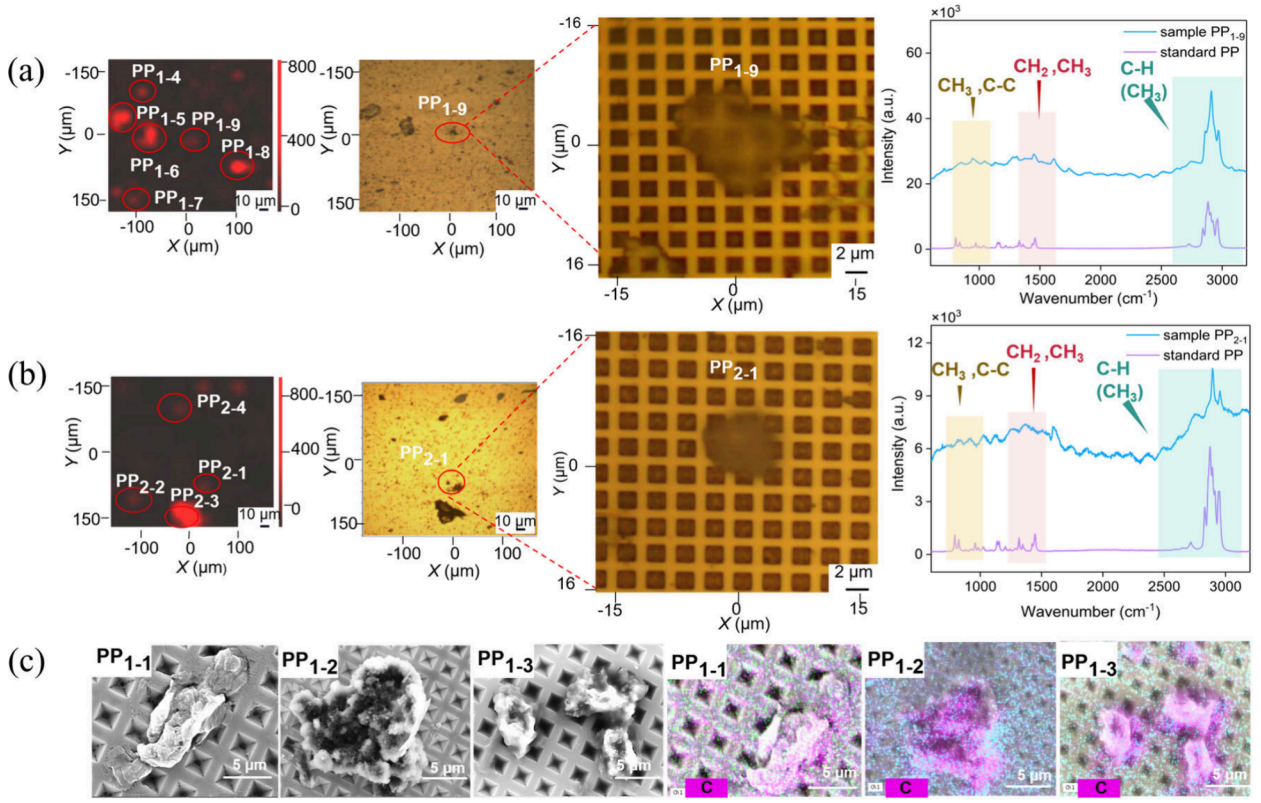

Figure 2. Detection of MPs and nanoplastics from intravenous injections. (a) Raman mapping image and optical, bright-field microscopic image (the squared area is mapped via the characteristic peak at 2800−3200 cm^{-1}) and the corresponding Raman spectrum after magnification (from the brand 1 sample). (b) Raman mapping image and optical, bright-field microscopic image (the squared area is mapped via the characteristic peak at 2800−3200 cm^{-1}) and the corresponding Raman spectrum after magnification (from the brand 2 sample). (c) SEM images and energy dispersive X-ray spectroscopy (EDS) map of PP particles (from PP plastic bottles). $PP_{1\text{-}1}$, filamentous; $PP_{1\text{-}2}$, block; $PP_{1\text{-}3}$, granular. EDS spectra correspond to the respective particles mentioned above.

infusion tube to mimic the intravenous infusion process in clinical settings. During the infusion process, the beaker was consistently covered with aluminum foil, preventing interference from other particles. Subsequently, the collected injection solution from the beaker was filtered using a vacuum filtration setup with a 0.2 μm polycarbonate membrane. The membrane after filtration was carefully picked up with the cleaned tweezer and placed in a beaker containing 10 mL of deionized water for infiltration, followed by 5 min of ultrasonication. The resulting samples were transferred in an oven at 50 °C for 4 h to be further concentrated to 1 mL. Finally, the concentrated samples were deposited using a glass pipet to a V-shaped Si−Au substrate, followed by drying for subsequent measurements.

The homemade V-shaped Si−Au substrate was applied as the surface-enhanced substrate for Raman detection in medical devices. It possesses a well-organized, compact grid structure comprising cavities, or "pits", configured as inverted pyramids. Each pit structure has a depth of approximately 1.77 μm. Notably, on the inverted pyramid structure of the gold-sprayed substrate, clear Raman signals of individual PP particles are readily detected.

2.3. Experimental Setup and Procedure

PP infusion bottles are common on the market because of their transparency, chemical corrosion resistance, and sealing properties.[34,35] For our study, we selected two types of intravenous infusion bottles (brand 1 and brand 2), each containing 250 mL of saline solution (salt water that contains 0.9% salt, matching the salt and water composition of human blood). The fluid was extracted at a flow rate of 40−60 drops/min, corresponding to an injection flow rate commonly used in hospitals. The fluid was then filtered using polycarbonate filter paper (0.2 μm) purchased from Whatman. Subsequently, the filtrate was collected and concentrated prior to oven-drying and transferred onto a custom-made SERS substrate; see Figure 1a. Our method was previously demonstrated as a successful tool for investigating MPs in human tissue and in rainwater.[36,37]

The SERS substrate is key for identifying and characterizing the detected particles. Given their small size, MPs present very weak intrinsic Raman signals. To enlarge these signals, our SERS substrate employs inverted-pyramid-shaped nanostructures; see Figure 1b. The substrate is made of Si, with each pit measuring 1.5 × 1.5 μm^2, and it is covered with a Au layer. It is the surface plasmon resonance and the lightning rod effect at the edges of the inverted-pyramid shapes that serve to concentrate the electric field of light and ensure the SERS effect. In the process, the detection limit for MPs is lowered, considerably.[38] Figure 1c presents the Raman spectrum from the bottles themselves. As expected, this spectrum matches the well-known spectrum of PP and serves as a reference signal for our study. Our hypothesis is that the PP bottles are the source of MPs in the fluid.

2.4. Morphology Analysis and Composition Characterization

Scanning electron microscopy coupled with energy-dispersive spectroscopy (SEM-EDS) was conducted to characterize the MPs. The SEM-EDS analysis was performed using a TESCAN VEGA3 scanning electron microscope (Shanghai Life Science International Trading Co., Ltd.). Instrument model: VEGA3SBU0304070202. A V-shaped Si−Au substrate coated with the prepared sample was mounted on the platform with a conductive adhesive. Measurements were carried out using a 15 kV beam, and the collected SEM images were further analyzed to determine the length and width of PP MP samples and their size distribution accordingly. Specifically, the resulting samples, after filtration, were first dispersed into ethanol solvent in an ultrasonication bath for 10 min. In the subsequent step, one or two drops of the dispersed sample were deposited onto the V-shaped Si−

https://doi.org/10.1021/envhealth.4c00210
Environ. Health 2025, 3, 551−559

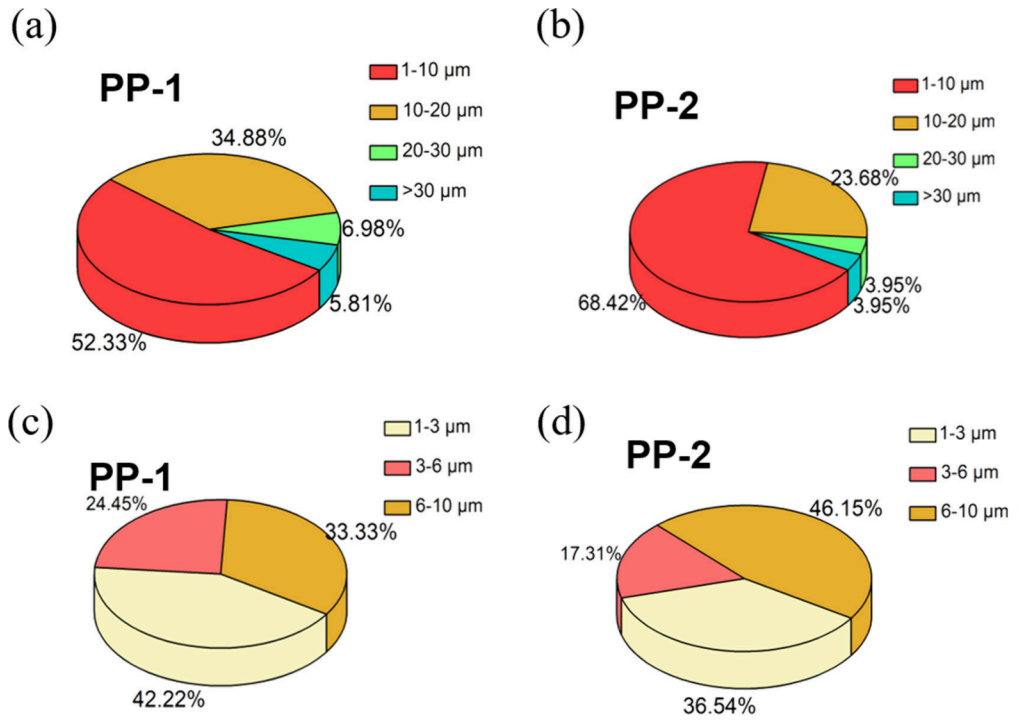

Figure 3. Size distributions of the PP particles extracted from intravenous fluid bottles. (a and c) Size distribution of the PP particles from brand 1 infusion bottles in two different ranges. (b and d) The corresponding size distributions for brand 2.

Au substrate. After air-drying, the samples were examined by using SEM-EDS equipment.

2.5. Raman Measurement and Data Analysis

We employed an XploRA Plus confocal Raman spectrometer, manufactured by Horiba Jobin Yvon, for Raman spectroscopy analysis. The spectrometer was equipped with a 100× objective lens (Olympus, numerical aperture of 0.90) and a 50 mW, 532 nm solid-state laser. The diffraction grating had a density of 1200 gr/mm, with a wavelength of 532 nm. The spectroscopic signals were collected using a thermoelectrically cooled open-electrode charge-coupled device (CCD) detector, with a minimum of 1024 pixels and a maximum full-width at half-maximum (FWHM) of 1.4 cm^{-1}.

Prior to the experiment, a calibration of the Raman signal was performed using a silicon wafer ((110) crystal face) at 520.7 cm^{-1} for the Stokes Raman signal of pure Si. During single-point measurements, the spectral range collected was from 600 to 3200 cm^{-1} with 40 spectra accumulations and a 3 s acquisition time per spectrum. Raman mapping imaging was conducted by performing single-point measurements within a selected area, using the same acquisition parameters as the single-point measurements (positive MPs were set to red, and the background was set to black).[39] The laboratory-simulated sample had a step size of 11.3 μm. All acquired Raman data were processed by using commercial software LabSpec 6.0.

In addition to detecting signals from individual particles in the infusion solution, we applied the software "ImageJ" to determine the particle sizes of the MPs identified by the Raman image.

2.6. Quality Assurance and Quality Control

Experiments were carried out in a high cleanliness laboratory with latex gloves and plastic-free fiber lab coats worn throughout to avoid collecting unwanted particles. Pipette tips, etc. were made of glass (Nichiryo), and all glass instruments were sonicated three times with ultrapure water (Direct-Q) for five min each time, interspersed with three rinses. All glass containers used in the experiment were washed three times with ultrapure water, covered with aluminum foil, and stored until the next use to prevent contamination of the surrounding environment.

2.7. Quantification of PP Particles

We examined six random regions (each with an area S_1 of 340 × 340 μm^2) of the whole sample, while the total area of the sample (S_t) was 4000 × 4000 μm^2. The average number of 250 mL bottles injected per person per year is represented by Q. The average particle count obtained from the six regions is denoted as N_1, while the overall average number of particles entering the human body annually through infusion is denoted as N_t.

$$N_t = \frac{S_t}{6S_1} \times N_1 \times Q \quad (1)$$

3. RESULTS AND DISCUSSION

3.1. Detection of MPs from Intravenous Injections

The presence of MPs in the fluid is unambiguously established in Figure 2. Figure 2a shows wide-field optical reflection microscopy and Raman imaging of the SERS substrate. Several particles are readily observed. They are labeled $PP_{x\text{-}y}$, indicating PP particle from the bottle of brand x with particle number y. $PP_{1\text{-}9}$ is a representative example, and its Raman spectrum matches well the reference PP spectrum in Figure 1c (reproduced here for the sake of convenience). Specifically, the characteristic peak at 965 cm^{-1} corresponds to the CH_3 rocking and C−C stretching vibrations. Additionally, the prominent peak at 1480 cm^{-1} is associated with the bending vibrations of CH_2 and CH_3.[40] Signals observed at 2843, 2895, and 2987 cm^{-1} can be attributed to the stretching vibrations of C−H (CH_3) bonds. The prominent peak at 1480 cm^{-1} can be attributed to the bending vibrations of CH_2 and CH_3 groups, and those signals observed at 2832, 2900, and 2990 cm^{-1} are indicative of the stretching vibrations of C−H (CH_3) bonds.

The presence of PP particles in the liquid is not brand-specific. As Figure 2b illustrates, particles were observed also from brand 2. Moreover, all the above-mentioned, well-known Raman spectral features were also revealed in these particles, as

https://doi.org/10.1021/envhealth.4c00210
Environ. Health 2025, 3, 551−559

exemplified by $PP_{2\text{-}1}$.[41,42] Further evidence is provided in Figure S1.

To gain more insight into the particle morphology, SEM and EDS images are provided in Figure 2c. EDS reveals that the primary elemental constituent of these particles is carbon, as expected for PP.[43] Moreover, the shape of the particles is irregular, which is not unexpected for PP. As Figure 2c illustrates, we can distinguish filamentous particles with an approximate size of 15 μm, block-like particles, and granular particles with sizes approaching 5 μm (Figure 2c). More SEM images are given in Figures S2 and S3.

3.2. Determination of Size Distribution and Quantification of PP MPs

To investigate the distribution of particle sizes, we measured the contents of six 250 mL infusion bottles, three from brand 1 and three from brand 2. Following filtration, the particles from these bottles were deposited on six corresponding SERS substrates, each with an area of 4000 × 4000 μm^2. From each SERS substrate, a random region of 340 × 340 μm^2 was Raman mapped to confirm the PP composition of the particles. Each confirmed particle was then counted and measured. This procedure resulted in six tables with individual particle measurements; see Tables S1 and S2. According to their size (measured across the longest end-to-end), the particles were classified into six groups: 1−3, 3−6, 6−10, 10−20, 20−30, and >30 μm. The results are summarized in Figure 3. We find that the particles range from 1 to 62 μm. For brand 1, over 52% of the PP particles were in the size range of 1−10 μm, followed by 35% and 7% in that of 10−20 μm and 20−30 μm, respectively, with the lowest abundance determined for the particles larger than 30 μm in size. A similar distribution was recorded for brand 2, with over 68% of particles ranging from 1 to 10 μm, followed by 24% in the size range of 10−20 μm. Figure 3 also shows the size distributions in the 1 to 10 μm range. These data allowed us to estimate the concentrations of PP particles in each bottle.

PP particle concentration was calculated by establishing the particle surface density on each one of the six measured 340 × 340 μm^2 areas. For instance, under measurement 1 in Table S1, there are 80 identified and measured PP particles. The corresponding particle surface density is $80/(340 \times 340)$ particles/μm^2. Therefore, we can estimate the total number of particles on the 4000 × 4000 μm^2 SERS substrate at ∼1846. All six particle number estimates are provided in Table S3. We found a narrow distribution of counts. For brand 1 and brand 2, the mean numbers of particles are ∼1977 and ∼1754, respectively. We conducted blank measurements and randomly selected 10 regions (160 × 126 μm^2) and five magnified regions (30 × 30 μm^2) under SEM for analysis. No interfering particles were observed, ensuring that our quantitative results remain unaffected. More details can be seen in Figure S4. Given the 250 mL volume of each bottle, the corresponding particle concentrations are ∼7900 and ∼7020 particles/L. In the following, we will take an average of 7500 particles/L. Who is likely to receive these particles?

3.3. Human Health Risks Associated with Intravenous Exposure to MPs

Almost all hospitalized patients require hydration and diluents for drug administration, both of which are provided by intravenous fluids.[44] Crystalloid fluids (such as normal saline, Ringer's lactate, and Hartmann's solution) are among the most commonly used fluids worldwide, typically available in 0.5 and 1 L polymer bottles. Dehydration is defined as the loss of over 2% of body weight, and severe dehydration is defined as the loss of over 7% of body weight.[45] With an estimated average human weight of 60 to 80 kg, severe dehydration requires replacing 4.2 to 5.6 L of water, which could correspond to between 31,500 and 42,000 particles per person. Intravenous treatment can also be indicated in cases such as exertional heat illness, nausea, emesis, or diarrhea, as well as in cases where patients cannot ingest oral fluids.[46] Assuming an average weight of 65 kg, intravenous fluid therapy (13−16 bottles of 250 mL 0.9% NaCl in 1 day) is required for hospitalized patients to maintain fluid balance,[47] which could correspond to 24,375 to 30,000 particles. During abdominal surgery, ∼7 L of fluid is administrated to each patient on the day of the surgery,[48] which amounts to up to 52,500 PP particles in the blood of each patient. Dehydration is particularly important during labor and especially during prolonged labor.

A study on the importance of intravenous hydration found that mothers could receive ∼240 mL/h during labor of ∼4.1 h,[49] which could correspond to ∼7380 particles in the bloodstream of the laboring mothers. Furthermore, to correct hypotensive shock, rapid infusion of at least 500 mL of fluid is required, which corresponds to 3750 particles administered in 15 min. During fluid resuscitation, 0.5 to 1 L of crystalloid fluid is infused, which would correspond to a dose of up to 7500 particles in 30 min.[50,51] Beyond hospitals, hydration by infusion is sometimes practiced in sports, where large sweat rates are defined as >1.5 L/h.[52] These rates would correspond to 11,250 particles/h. Next, we must consider the consequences of particles being injected into the human bloodstream.

MPs have already been clearly identified in human blood.[9] As further evidence, in a recent study, plaque was removed from the carotid arteries of 304 individuals and PE was detected in the plaque of 58.4% of the patients.[53] Patients with detected polymers in their plaque were found to be at >4.5 times higher risk for a fatal event (over the 34 months follow-up). Additionally, a recent study investigated the presence of MPs in human thrombus (a pathological structure formed within blood vessels).[41] Twenty-six thrombi were examined, and 16 contained particles, that ranged in size from 2.1 to 26.0 μm, with 69% of particles being smaller than 10 μm. The majority of particles identified were pigments and iron compounds, but the presence of MPs (PE) was also confirmed. From blood, MPs can also be deposited inside the organs.

MPs injected into the bloodstream have been observed to accumulate in organs, such as the lungs, liver, kidneys, and spleen. However, although these findings suggest the potential for MPs to interact with these organs, the exact mechanisms and causality remain unclear and require further investigation. Polystyrene microspheres with diameters 1.27 and 15.8 μm, as well as cellulose microspheres with diameters 40−160 μm, were injected into the bloodstream of rabbits, and the organ deposition was studied.[54] The 1.27 μm particles were localized mainly in the liver but also in the spleen and lungs. The 15.8 μm particles were deposited mainly in the lungs, much fewer in the liver, and none in the spleen. The cellulose microspheres were also deposited in the lungs, with small quantities in the liver and kidney. In humans, MPs have been reported in several organs. In a study of 11 patients, six with end-stage liver cirrhosis and five without, MPs of six different polymers were found in the liver of patients with cirrhosis but not in the healthy patients.[55] The particles detected in the liver ranged

https://doi.org/10.1021/envhealth.4c00210
Environ. Health 2025, 3, 551−559

from 3.0 to 29.5 μm with a median of 9.8 μm compared to our median of 9.2 μm (brand 1) and 7.7 μm (brand 2). Furthermore, the human placenta has been shown to be permeable to PP particles, 5 to 10 μm in size.[56] What is the impact of such particles on the human body?

Particulate matter inside intravenous solutions is considered hazardous contamination by the United States Pharmacopoeia (USP) and the European Pharmacopoeia (EP).[57,58] While plastics are generally considered inert, their MPs can lead to deleterious physical and chemical effects.[59] The physical effects of MPs primarily depend on their size and shape. These particles may induce biological responses, such as inflammation, genotoxicity, apoptosis, and necrosis, which could potentially lead to tissue damage and fibrosis. However, the evidence regarding carcinogenesis remains limited, and further research is needed to clarify any potential relationship.[59] Other MPs (including drug precipitates, glass, rubber, etc.) with comparable size and shape have previously been identified in infusion fluids, and their detrimental effects have been reported.[28] In critically ill children, it has been reported that infused particles are associated with significant complications, such as inflammation or organ dysfunctions.[60] Lungs can be particularly affected by the intravenous administration of particles. This is easy to understand, given the size distributions we report—median of 9.2 μm (brand 1) and of 7.7 μm (brand 2) and that the mean diameter of pulmonary capillaries is approximately 2 to 15 μm.[60] An example of respiratory obstruction due to infused particles was reported by McNearney et al.[61] Following total parenteral nutrition (TPN) (a method of providing nutrition directly into the bloodstream intravenously), a 26-year-old woman presented fever (up to 38.9 °C) and shortness of breath (88−91% oxygen saturation in room air). A lung biopsy revealed widespread blood clots (thromboses) in artery branches, damage to the blood vessels, and the formation of granulomas (immune cells encapsulated in fibrous tissue). The cause was particulate matter ranging from 0.5 to 650 μm; upon discontinuing the TPN, the patient recovered. Because of their trigger coagulation, infused particles could also lead to organ malfunction; for instance, during cardiac surgery.[29] Chemical effects are due to the composition of the polymers. Accordingly, MPs can decompose to monomers and release undesirable chemicals, added during their production processes, such as plasticizers. Such chemicals can be toxic and can trigger a localized immune response.[59]

4. CONCLUSIONS

In summary, our findings highlight an aspect of plastic pollution that affects humans most directly, as MPs are being injected into the bloodstream. This pathway was identified years before the landmark report on the effects of plastic pollution on marine life; yet, it has received much less attention. We found that, after filtering, infusion solutions from PP bottles contain approximately 7500 particles/L. The particles ranged in size from 1 to 62 μm, with ∼90% of particles between 1 and 20 μm in size and ∼60% of the particles in the range 1 to 10 μm. We note that our estimations are based on quantitative results obtained from laboratory-based experiments in a controlled environment. Hence, there are further factors that need to be considered in follow-up studies, such as variations between additional brands, batch discrepancies, disparities across manufacturing facilities, disparities in PP quality, postproduction duration dependencies, and dependencies on storage conditions. Especially important conditions are temperature and UV light exposure. UV radiation is known to catalyze the photo-oxidation of plastics, causing them to become brittle. Moreover, when the temperature rises from 23 to 40 °C, the stiffness of PP (and that of other common polymers) decreases by 20%. All of these factors affect the degradation of plastics into MPs. MPs in infusion products primarily originate from raw materials and packaging components, requiring strict quality control to ensure compliance with pharmacopeial standards and to avoid insoluble particles. Potentially effective measures include the use of highly efficient micrometer- or submicrometer-level filtration systems during intravenous infusion and enhanced monitoring across the medical device and pharmaceutical supply chain to meet stringent safety standards. Additionally, innovative infusion system designs using materials resistant to MP shedding and optimized closed systems may significantly minimize external contamination. Future research should focus on more direct toxicological studies to comprehensively assess the potential toxicity of MPs and their associated health risks. These findings will provide a scientific basis for formulating appropriate policies and measures to mitigate the potential threats posed by MPs to human health.

■ ASSOCIATED CONTENT

Supporting Information

The Supporting Information is available free of charge at https://pubs.acs.org/doi/10.1021/envhealth.4c00210.

Raman spectra of PP from brands 1 and 2 (Figure S1), SEM images and EDS map of PP (from plastic bottle 2) (Figure S2), SEM images about brand 1 and brand 2 (Figure S3), SEM images of 10 regions and five magnified regions in the blank sample (Figure S4), the data on the size distribution of PP particles in brand 1 (obtained through three repeated experiments) (Table S1), the data on the size distribution of PP particles in brand 2 (obtained through three repeated experiments) (Table S2), and the particle counts (PP) and standard deviations for three experiments of the two brands (Table S3) (PDF)

■ AUTHOR INFORMATION

Corresponding Authors

Liwu Zhang − *Shanghai Key Laboratory of Atmospheric Particle Pollution and Prevention, National Observations and Research Station for Wetland Ecosystems of the Yangtze Estuary, IRDR International Center of Excellence on Risk Interconnectivity and Governance on Weather, Department of Environmental Science & Engineering, Fudan University, Shanghai 200433, China; Shanghai Institute of Pollution Control and Ecological Security, Shanghai 200092, China;* orcid.org/0000-0002-0765-8660; Email: zhanglw@fudan.edu.cn

Ventsislav Kolev Valev − *Centre for Photonics and Photonic Materials and Centre for Nanoscience and Nanotechnology, Department of Physics, University of Bath, Bath BA2 7AY, United Kingdom*; Email: vkv23@bath.ac.uk

Authors

Tingting Huang − *Shanghai Key Laboratory of Atmospheric Particle Pollution and Prevention, National Observations and Research Station for Wetland Ecosystems of the Yangtze*

Estuary, IRDR International Center of Excellence on Risk Interconnectivity and Governance on Weather, Department of Environmental Science & Engineering, Fudan University, Shanghai 200433, China; Shanghai Institute of Pollution Control and Ecological Security, Shanghai 200092, China

Yangyang Liu − *Shanghai Key Laboratory of Atmospheric Particle Pollution and Prevention, National Observations and Research Station for Wetland Ecosystems of the Yangtze Estuary, IRDR International Center of Excellence on Risk Interconnectivity and Governance on Weather, Department of Environmental Science & Engineering, Fudan University, Shanghai 200433, China; Shanghai Institute of Pollution Control and Ecological Security, Shanghai 200092, China*

Licheng Wang − *Shanghai Key Laboratory of Atmospheric Particle Pollution and Prevention, National Observations and Research Station for Wetland Ecosystems of the Yangtze Estuary, IRDR International Center of Excellence on Risk Interconnectivity and Governance on Weather, Department of Environmental Science & Engineering, Fudan University, Shanghai 200433, China; Shanghai Institute of Pollution Control and Ecological Security, Shanghai 200092, China*

Xuejun Ruan − *Shanghai Key Laboratory of Atmospheric Particle Pollution and Prevention, National Observations and Research Station for Wetland Ecosystems of the Yangtze Estuary, IRDR International Center of Excellence on Risk Interconnectivity and Governance on Weather, Department of Environmental Science & Engineering, Fudan University, Shanghai 200433, China; Shanghai Institute of Pollution Control and Ecological Security, Shanghai 200092, China*

Qiuyue Ge − *Shanghai Key Laboratory of Atmospheric Particle Pollution and Prevention, National Observations and Research Station for Wetland Ecosystems of the Yangtze Estuary, IRDR International Center of Excellence on Risk Interconnectivity and Governance on Weather, Department of Environmental Science & Engineering, Fudan University, Shanghai 200433, China; Shanghai Institute of Pollution Control and Ecological Security, Shanghai 200092, China*

Minglu Ma − *Shanghai Key Laboratory of Atmospheric Particle Pollution and Prevention, National Observations and Research Station for Wetland Ecosystems of the Yangtze Estuary, IRDR International Center of Excellence on Risk Interconnectivity and Governance on Weather, Department of Environmental Science & Engineering, Fudan University, Shanghai 200433, China; Shanghai Institute of Pollution Control and Ecological Security, Shanghai 200092, China*

Wei Wang − *Shanghai Key Laboratory of Atmospheric Particle Pollution and Prevention, National Observations and Research Station for Wetland Ecosystems of the Yangtze Estuary, IRDR International Center of Excellence on Risk Interconnectivity and Governance on Weather, Department of Environmental Science & Engineering, Fudan University, Shanghai 200433, China; Shanghai Institute of Pollution Control and Ecological Security, Shanghai 200092, China*

Wenbo You − *Shanghai Key Laboratory of Atmospheric Particle Pollution and Prevention, National Observations and Research Station for Wetland Ecosystems of the Yangtze Estuary, IRDR International Center of Excellence on Risk Interconnectivity and Governance on Weather, Department of Environmental Science & Engineering, Fudan University, Shanghai 200433, China; Shanghai Institute of Pollution Control and Ecological Security, Shanghai 200092, China*

Liwen Zhang − *Intensive Care Unit, Affiliated Hospital of Jining Medical University, Jining 272100 Shandong Province, China*

Complete contact information is available at: https://pubs.acs.org/10.1021/envhealth.4c00210

Author Contributions

#T.H., Y.L., L.W., and X.R. contributed equally to this work. T.H. and Y.L. designed and built the experimental set-ups, maintained the experimental apparatus, and carried out the experiments. T.H., Y.L., V.K.V., L.W., and X.R. analyzed the experimental data. All authors discussed and interpreted the data. T.H. and Y.L. wrote the paper with input from all authors.

Notes

The authors declare no competing financial interest.

■ ACKNOWLEDGMENTS

The authors gratefully acknowledge financial support from the National Natural Science Foundation of China (22376028, 22176036, 21976030, and 22006020).

■ REFERENCES

(1) Revell, L. E.; Kuma, P.; Le Ru, E. C.; Somerville, W. R. C.; Gaw, S. Direct radiative effects of airborne microplastics. *Nature* **2021**, *598* (7881), 462−467.

(2) Kahane-Rapport, S. R.; Czapanskiy, M. F.; Fahlbusch, J. A.; Friedlaender, A. S.; Calambokidis, J.; Hazen, E. L.; Goldbogen, J. A.; Savoca, M. S. Field measurements reveal exposure risk to microplastic ingestion by filter-feeding megafauna. *Nat. Commun.* **2022**, *13* (1), 6327.

(3) Evangeliou, N.; Grythe, H.; Klimont, Z.; Heyes, C.; Eckhardt, S.; Lopez-Aparicio, S.; Stohl, A. Atmospheric transport is a major pathway of microplastics to remote regions. *Nat. Commun.* **2020**, *11* (1), 3381.

(4) Peeken, I.; Primpke, S.; Beyer, B.; Gutermann, J.; Katlein, C.; Krumpen, T.; Bergmann, M.; Hehemann, L.; Gerdts, G. Arctic sea ice is an important temporal sink and means of transport for microplastic. *Nat. Commun.* **2018**, *9* (1), 1505.

(5) Kane, I. A.; Clare, M. A.; Miramontes, E.; Wogelius, R.; Rothwell, J. J.; Garreau, P.; Pohl, F. Seafloor microplastic hotspots controlled by deep-sea circulation. *Science* **2020**, *368* (6495), 1140−1145.

(6) Allen, S.; Allen, D.; Baladima, F.; Phoenix, V. R.; Thomas, J. L.; Le Roux, G.; Sonke, J. E. Evidence of free tropospheric and long-range transport of microplastic at Pic du Midi Observatory. *Nat. Commun.* **2021**, *12* (1), 7242.

(7) Carpenter, E. J.; Anderson, S. J.; Harvey, G. R.; Miklas, H. P.; Peck, B. B. Polystyrene Spherules in Coastal Waters. *Science* **1972**, *178* (4062), 749−750.

(8) Seeley, M. E.; Song, B.; Passie, R.; Hale, R. C. Microplastics affect sedimentary microbial communities and nitrogen cycling. *Nat. Commun.* **2020**, *11* (1), 2372.

(9) Dąbrowska, A.; Mielańczuk, M.; Syczewski, M. The Raman spectroscopy and SEM/EDS investigation of the primary sources of microplastics from cosmetics available in Poland. *Chemosphere* **2022**, *308*, 136407.

(10) Zhou, Y.; Ashokkumar, V.; Amobonye, A.; Bhattacharjee, G.; Sirohi, R.; Singh, V.; Flora, G.; Kumar, V.; Pillai, S.; Zhang, Z.; Awasthi, M. K. Current research trends on cosmetic microplastic pollution and its impacts on the ecosystem: A review. *Environ. Pollut.* **2023**, *320*, 121106.

(11) Mitrano, D. M.; Wohlleben, W. Microplastic regulation should be more precise to incentivize both innovation and environmental safety. *Nat. Commun.* **2020**, *11* (1), 5324.

(12) Simon, M.; van Alst, N.; Vollertsen, J. Quantification of microplastic mass and removal rates at wastewater treatment plants applying Focal Plane Array (FPA)-based Fourier Transform Infrared (FT-IR) imaging. *Water Res.* **2018**, *142*, 1−9.
(13) Jia, B.; Zhu, K.; Bai, Z.; Abudula, A.; Liu, B.; Yan, J.; Wu, Z.; Tan, H.; Liu, Q.; Morawska, L.; Wang, L.; Chen, J. Non targeted and targeted LC-MS/MS insights into the composition and concentration of atmospheric microplastics and additives: Impacts and regional changes of sandstorms in Shanghai and Hohhot, China. *Sci. Total. Envrion.* **2024**, *953*, 176254.
(14) Li, P.; Li, Q.; Lai, Y.; Yang, S.; Yu, S.; Liu, R.; Jiang, G.; Liu, J. Direct entry of micro(nano)plastics into human blood circulatory system by intravenous infusion. *iScience* **2023**, *26* (12), 108454.
(15) Kim, J. Y.; Koh, E. H.; Yang, J.-Y.; Mun, C.; Lee, S.; Lee, H.; Kim, J.; Park, S.-G.; Kang, M.; Kim, D.-H.; Jung, H. S. 3D Plasmonic Gold Nanopocket Structure for SERS Machine Learning-Based Microplastic Detection. *Adv. Funct. Mater.* **2024**, *34* (2), 2307584.
(16) Chen, Q.; Wang, J.; Yao, F.; Zhang, W.; Qi, X.; Gao, X.; Liu, Y.; Wang, J.; Zou, M.; Liang, P. A review of recent progress in the application of Raman spectroscopy and SERS detection of microplastics and derivatives. *Microchim. Acta* **2023**, *190* (12), 465.
(17) Caldwell, J.; Taladriz-Blanco, P.; Rodriguez-Lorenzo, L.; Rothen-Rutishauser, B.; Petri-Fink, A. Submicron- and nanoplastic detection at low micro- to nanogram concentrations using gold nanostar-based surface-enhanced Raman scattering (SERS) substrates. *Environ. Sci. Nano.* **2024**, *11* (3), 1000−1011.
(18) Isobe, A.; Iwasaki, S.; Uchida, K.; Tokai, T. Abundance of non-conservative microplastics in the upper ocean from 1957 to 2066. *Nat. Commun.* **2019**, *10* (1), 417.
(19) Rillig, M. C.; Lehmann, A. Microplastic in terrestrial ecosystems. *Science* **2020**, *368* (6498), 1430−1431.
(20) Ramsperger, A. F. R. M.; Narayana, V. K. B.; Gross, W.; Mohanraj, J.; Thelakkat, M.; Greiner, A.; Schmalz, H.; Kress, H.; Laforsch, C. Environmental exposure enhances the internalization of microplastic particles into cells. *Sci. Adv.* **2020**, *6* (50), No. eabd1211.
(21) Kadac-Czapska, K.; Knez, E.; Grembecka, M. Food and human safety: the impact of microplastics. *Crit. Rev. Food Sci. Nutr.* **2024**, *64*, 3502.
(22) Guo, X.; Dai, H.; Gukowsky, J.; Tan, X.; He, L. Detection and quantification of microplastics in commercially bottled edible oil. *Food Packag. Shelf Life* **2023**, *38*, 101122.
(23) Jenner, L. C.; Rotchell, J. M.; Bennett, R. T.; Cowen, M.; Tentzeris, V.; Sadofsky, L. R. Detection of microplastics in human lung tissue using muFTIR spectroscopy. *Sci. Total. Envrion.* **2022**, *831*, 154907.
(24) Baeza-Martinez, C.; Olmos, S.; Gonzalez-Pleiter, M.; Lopez-Castellanos, J.; Garcia-Pachon, E.; Masia-Canuto, M.; Hernandez-Blasco, L.; Bayo, J. First evidence of microplastics isolated in European citizens' lower airway. *J. Hazard Mater.* **2022**, *438*, 129439.
(25) Zhao, J.; Lan, R.; Wang, Z.; Su, W.; Song, D.; Xue, R.; Liu, Z.; Liu, X.; Dai, Y.; Yue, T.; Xing, B. Microplastic fragmentation by rotifers in aquatic ecosystems contributes to global nanoplastic pollution. *Nat. Nanotechnol.* **2024**, *19* (3), 406−414.
(26) Pivokonsky, M.; Cermakova, L.; Novotna, K.; Peer, P.; Cajthaml, T.; Janda, V. Occurrence of microplastics in raw and treated drinking water. *Sci. Total. Envrion.* **2018**, *643*, 1644−1651.
(27) Davis, N. M.; Turco, S.; Sivelly, E. A Study of Particulate Matter in I.V. Infusion Fluids. *Am. J. Hosp. Pharm.* **1970**, *27* (10), 822−826.
(28) Turco, S. J.; Davis, N. M. Detrimental Effects of Particulate Matter on the Pulmonary Circulation. *JAMA* **1971**, *217* (1), 81−82.
(29) Sasse, M.; Dziuba, F.; Jack, T.; Köditz, H.; Kaussen, T.; Bertram, H.; Beerbaum, P.; Boehne, M. In-line Filtration Decreases Systemic Inflammatory Response Syndrome, Renal and Hematologic Dysfunction in Pediatric Cardiac Intensive Care Patients. *Pediatr. Cardiol.* **2015**, *36* (6), 1270−1278.
(30) Leslie, H. A.; van Velzen, M. J. M.; Brandsma, S. H.; Vethaak, A. D.; Garcia-Vallejo, J. J.; Lamoree, M. H. Discovery and quantification of plastic particle pollution in human blood. *Environ. Int.* **2022**, *163*, 107199.
(31) Zhu, L.; Ma, M.; Sun, X.; Wu, Z.; Yu, Y.; Kang, Y.; Liu, Z.; Xu, Q.; An, L. Microplastics Entry into the Blood by Infusion Therapy: Few but a Direct Pathway. *Environ. Sci. Technol. Lett.* **2024**, *11* (2), 67−72.
(32) Gopinath, P. M.; Parvathi, V. D.; Yoghalakshmi, N.; Kumar, S. M.; Athulya, P. A.; Mukherjee, A.; Chandrasekaran, N. Plastic particles in medicine: A systematic review of exposure and effects to human health. *Chemosphere* **2022**, *303*, 135227.
(33) Schmitt, E.; Meybohm, P.; Herrmann, E.; Ammersbach, K.; Endres, R.; Lindau, S.; Helmer, P.; Zacharowski, K.; Neb, H. In-line filtration of intravenous infusion may reduce organ dysfunction of adult critical patients. *Crit. Care.* **2019**, *23* (1), 373.
(34) Guichard, N.; Bonnabry, P.; Rudaz, S.; Fleury-Souverain, S. Stability of busulfan solutions in polypropylene syringes and infusion bags as determined with an original assay. *Am. J. Health-Syst. Pharm.* **2017**, *74* (22), 1887−1894.
(35) Kim, S. J.; Lee, J. W.; Kang, H. Y.; Kim, S. Y.; Shin, Y. K.; Kim, K. W.; Oh, J. S.; Lim, K. J.; Kim, J. Y. In-Use Physicochemical and Biological Stability of the Trastuzumab Biosimilar CT-P6 Upon Preparation for Intravenous Infusion. *BioDrugs* **2018**, *32* (6), 619−625.
(36) Xu, G.; Cheng, H.; Jones, R.; Feng, Y.; Gong, K.; Li, K.; Fang, X.; Tahir, M. A.; Valev, V. K.; Zhang, L. Surface-Enhanced Raman Spectroscopy Facilitates the Detection of Microplastics < 1 mum in the Environment. *Environ. Sci. Technol.* **2020**, *54* (24), 15594−15603.
(37) Ao, J.; Xu, G.; Wu, H.; Xie, L.; Liu, J.; Gong, K.; Ruan, X.; Han, J.; Li, K.; Wang, W.; Chen, T.; Ji, M.; Zhang, L. Fast detection and 3D imaging of nanoplastics and microplastics by stimulated Raman scattering microscopy. *Cell Rep. Phys. Sci.* **2023**, *4* (10), 101623.
(38) Fu, Y.; Kuppe, C.; Valev, V. K.; Fu, H.; Zhang, L.; Chen, J. Surface-Enhanced Raman Spectroscopy: A Facile and Rapid Method for the Chemical Component Study of Individual Atmospheric Aerosol. *Environ. Sci. Technol.* **2017**, *51* (11), 6260−6267.
(39) Sobhani, Z.; Al Amin, M.; Naidu, R.; Megharaj, M.; Fang, C. Identification and visualisation of microplastics by Raman mapping. *Anal. Chim. Acta* **2019**, *1077*, 191−199.
(40) Luo, Y.; Su, W.; Xu, D.; Wang, Z.; Wu, H.; Chen, B.; Wu, J. Component identification for the SERS spectra of microplastics mixture with convolutional neural network. *Sci. Total. Envrion.* **2023**, *895*, 165138.
(41) Li, F.; Liu, D.; Guo, X.; Zhang, Z.; Martin, F. L.; Lu, A.; Xu, L. Identification and visualization of environmental microplastics by Raman imaging based on hyperspectral unmixing coupled machine learning. *J. Hazard Mater.* **2024**, *465*, 133336.
(42) Lou, B. B.; Liu, Y. F.; Shi, M. L.; Chen, J.; Li, K.; Tan, Y. F.; Chen, L. W.; Wu, Y. W.; Wang, T.; Liu, X. Q.; Jiang, T.; Peng, D. M.; Liu, Z. B. Aptamer-based biosensors for virus protein detection. *TrAC Trends Anal. Chem.* **2022**, *157*, 116738.
(43) Montano, L.; Giorgini, E.; Notarstefano, V.; Notari, T.; Ricciardi, M.; Piscopo, M.; Motta, O. Raman Microspectroscopy evidence of microplastics in human semen. *Sci. Total. Envrion.* **2023**, *901*, 165922.
(44) Finfer, S.; Myburgh, J.; Bellomo, R. Intravenous fluid therapy in critically ill adults. *Nat. Rev. Nephrol.* **2018**, *14* (9), 541−557.
(45) Shephard, R.J. American College of Sports Medicine position stand: Exercise and fluid replacement. *Med. Sci. Sports. Exerc.* **2007**, *39* (2), 377−90.
(46) Givan, G. V.; Diehl, J. J. Intravenous Fluid Use in Athletes. *Sports Health* **2012**, *4* (4), 333−339.
(47) Intravenous fluid therapy in adults in hospital, Clinical Guideline CG174. *National Institute for Health and Care Excellence*, 2017.
(48) Myles, P. S.; Bellomo, R.; Corcoran, T.; Forbes, A.; Peyton, P.; Story, D.; Christophi, C.; Leslie, K.; McGuinness, S.; Parke, R.; Serpell, J.; Chan, M. T. V.; Painter, T.; McCluskey, S.; Minto, G.; Wallace, S. Australian; New Zealand College of Anaesthetists Clinical Trials, N.; the, A.; New Zealand Intensive Care Society Clinical Trials,

G. Restrictive versus Liberal Fluid Therapy for Major Abdominal Surgery. *NEJM.* **2018**, *378* (24), 2263−2274.
(49) Direkvand-Moghadam, A.; Rezaeian, M. Increased intravenous hydration of nulliparas in labor. *Int. J. Gynecol. Obstet.* **2012**, *118* (3), 213−215.
(50) Taveras, L. R.; Jeschke, M. G.; Wolf, S. E. Critical Care in Burns. *Handbook of Burns Volume 1: Acute Burn Care* **2020**, 255−278.
(51) Frazee, E.; Kashani, K. Fluid Management for Critically Ill Patients: A Review of the Current State of Fluid Therapy in the Intensive Care Unit. *Kidney Diseases* **2016**, *2* (2), 64−71.
(52) Ganio, M. S.; Casa, D. J.; Armstrong, L. E.; Maresh, C. M. Evidence-Based Approach to Lingering Hydration Questions. *Clin. Sports. Med.* **2007**, *26* (1), 1−16.
(53) Marfella, R.; Prattichizzo, F.; Sardu, C.; Fulgenzi, G.; Graciotti, L.; Spadoni, T.; D'Onofrio, N.; Scisciola, L.; La Grotta, R.; Frigé, C.; Pellegrini, V.; Municinò, M.; Siniscalchi, M.; Spinetti, F.; Vigliotti, G.; Vecchione, C.; Carrizzo, A.; Accarino, G.; Squillante, A.; Spaziano, G.; Mirra, D.; Esposito, R.; Altieri, S.; Falco, G.; Fenti, A.; Galoppo, S.; Canzano, S.; Sasso, F. C.; Matacchione, G.; Olivieri, F.; Ferraraccio, F.; Panarese, I.; Paolisso, P.; Barbato, E.; Lubritto, C.; Balestrieri, M. L.; Mauro, C.; Caballero, A. E.; Rajagopalan, S.; Ceriello, A.; D'Agostino, B.; Iovino, P.; Paolisso, G. Microplastics and Nanoplastics in Atheromas and Cardiovascular Events. *NEJM.* **2024**, *390* (10), 900−910.
(54) Ilium, L.; Davis, S. S.; Wilson, C. G.; Thomas, N. W.; Frier, M.; Hardy, J. G. Blood clearance and organ deposition of intravenously administered colloidal particles. The effects of particle size, nature and shape. *Int. J. Pharm.* **1982**, *12* (2), 135−146.
(55) Horvatits, T.; Tamminga, M.; Liu, B.; Sebode, M.; Carambia, A.; Fischer, L.; Püschel, K.; Huber, S.; Fischer, E. K. Microplastics detected in cirrhotic liver tissue. *eBioMedicine* **2022**, *82*, 104147.
(56) Ragusa, A.; Svelato, A.; Santacroce, C.; Catalano, P.; Notarstefano, V.; Carnevali, O.; Papa, F.; Rongioletti, M. C. A.; Baiocco, F.; Draghi, S.; D'Amore, E.; Rinaldo, D.; Matta, M.; Giorgini, E. Plasticenta: First evidence of microplastics in human placenta. *Environ. Int.* **2021**, *146*, 106274.
(57) (788) Particulate Matters in Injections. *The United States Pharmacopoeia − National Formulary*, 2016.
(58) Particulate contamination: sub-visible particles. *The European Pharmacopoeia*, 9th ed.; 2016.
(59) Wright, S. L.; Kelly, F. J. Plastic and Human Health: A Micro Issue? *Environ. Sci. Technol.* **2017**, *51* (12), 6634−6647.
(60) Perez, M.; Décaudin, B.; Maiguy-Foinard, A.; Barthélémy, C.; Lebuffe, G.; Storme, L.; Odou, P. Dynamic Image Analysis To Evaluate Subvisible Particles During Continuous Drug Infusion In a Neonatal Intensive Care Unit. *Sci. Rep.* **2017**, *7* (1), 9404.
(61) McNearney, T.; Bajaj, C.; Boyars, M.; Cottingham, J.; Haque, A. CASE REPORT: Total Parenteral Nutrition Associated Crystalline Precipitates Resulting in Pulmonary Artery Occlusions and Alveolar Granulomas. *Dig. Dis. Sci.* **2003**, *48* (7), 1352−1354.

https://doi.org/10.1021/envhealth.4c00210
Environ. Health 2025, 3, 551−559